Thermophysics and Aeromechanics, *2020*, *Vol. 27*, *No. 2*

DOI: 10.1134/S0869864320020043

Stability of a supersonic boundary layer over a surface with sublimation*

S.A. Gaponov and B.V. Smorodsky

Khristianovich Institute of Theoretical and Applied Mechanics SB RAS, *Novosibirsk*, *Russia*

E-mail: gaponov@itam.nsc.ru

(*Received May 28*, *2019*; *revised May 28*, *2019*; *accepted for publication November 6*, *2019*)

The paper presents a theoretical study for a supersonic boundary layer over a flat plate in a stream of air at Mach number M = 2 under the conditions of surface sublimation. The sublimation-prone material is naphthalene ($C_{10}H_8$). Calculations demonstrated that at a higher surface temperature the mass flowrate of naphthalene evaporation is increasing. This reduces the wall temperature in comparison with a similar flow without sublimation. The high molecular mass of naphthalene (vs. air) and reduction of wall temperature due to the wall material evaporation creates a higher density of the binary gas mixture (air and naphthalene vapor) near the wall. This modification of the boundary layer profiles induces a significant reduction of instability growth rate. This fact was confirmed by calculations based on the linear stability theory. It was found that boundary layer stabilization occurs for growing sublimation surface temperature; it becomes a maximum near the triple point temperature of the coating material. The e^N method gives the estimates of the Reynolds number for laminar-turbulent transition. This shows a theoretical possibility of extension of the laminar boundary layer above a model with sublimation coating.

Keywords: supersonic boundary layer, laminar-turbulent transition, hydrodynamic stability, binary gas mixture, sublimation.

Introduction

Today, a need for studying at a boundary layer under conditions of surface ablation remains a topical problem. This is dictated by practical applications aimed at flight vehicle thermal protection (e.g., for a reentry space probe) by using air-thermo-chemically decaying protection coatings. The monograph [1] was focused on this subject: authors wrote that this kind of thermal protection for the pioneering series of space vehicles had been overestimated at those years because of insufficient knowledge about the thermal aspects of fluid dynamics. Onset of turbulence in a boundary layer is a significant factor for those aspects.

The problems related to a laminar-turbulent transition have been studied intensively worldwide in recent years. It is a common knowledge that for a situation of low external noise, this laminar-turbulent transition is caused by instability of the boundary layer. The foundations of the stability theory for a compressible boundary layer were formulated in 1950s. [2]. Further

* Research was performed in the framework of the Program for fundamental research for state academies of sciences in 2013-2020 (Project AAAA-A17-117030610125-7, No. 0323-2018-0009) and was also supported by Russian Foundation for Basic Research (Project No.18-01-00070-a) and by Russian Science Foundation (Project No. 17-19-01289).

evolution of research in the field of supersonic boundary stability was reflected in papers [3–5]. They were focused on boundary layers of a single-component gas.

The stability of a boundary layer with occurring chemical reactions was studied in papers [6, 7]. Those papers considered the stability of a boundary layer of nonequilibrium dissociating gas (like oxygen and nitrogen). Results were also discussed in book [8]. In more general form, the problem of stability of a hypersonic boundary layer with chemical reactions was studied in [9–14]. The flow stability and laminar-turbulent transition under conditions of material ablation was poorly studied yet. Up to now, only papers [15, 16] are known that deal with the stability of a hypersonic boundary layer (past a conical body) under the condition of mass ablation from the surface. These papers considered the case of only two-dimensional (2D) disturbances at very high Mach numbers: M = 16 and M = 20. However, these simulation results lacked a proper experimental validation. Therefore, further elaboration of a theoretical study initiated in those papers, but for the case of three-dimensional (3D) disturbances and moderate Mach number, would be important progress (here the theory can be proved by experiment).

The existing analytical and simulation studies indicate a possibility of qualitative prediction of flow stability and laminar-turbulent transition using simple features of the base-flow velocity and temperature profiles. Therefore, as the first step, our paper presents results of the sublimation influence on the parameters of a supersonic boundary layer. Then, these results are used for calculation of linear stability.

The high temperature ablation (typical of a real flight in atmosphere for a reentry vehicle) is a challenging phenomenon for reproduction under laboratory conditions. However, moderate-temperature sublimation can be realized in modern wind tunnels. This option enables studying of physical process of ablation under simplified conditions (no chemical reactions and other high temperature gas dynamic phenomena). In the present paper, we offer calculations of a laminar boundary layer and its linear stability for the case of naphthalene ($C_{10}H_8$) sublimation which occurs at moderate temperatures. As an example of using naphthalene in airflow physical experiments for a model with surface ablation, we can reference the paper [17]. It was demonstrated in [18] that using sublimation of naphthalene coating for visualization of laminar-turbulent transition in a swept-wing boundary layer is a robust experimental method. Visualization by means of laser-induced fluorescence of sublimating naphthalene vapor was used for the case of a turbulent boundary layer with the Mach number 5 [19] and it offered the 2D distribution of vapor concentration in the boundary layer.

The surface sublimation provides an injection of a foreign gas (sublimation vapor) into the boundary layer. Therefore, the boundary layer is no more component layer: this should be considered as a binary-mixture gas flow. The early papers of the authors on the subject of stability of a supersonic boundary layer for binary-mixture gas flow [20–24] demonstrated that injection of a heavy foreign-gas (with molecular weight higher than for the air) into a near-wall sublayer of the boundary layer through a permeable (porous) surface is beneficial for sustaining of boundary layer stability. These theoretical findings were confirmed later in experiments on stability and transition. The tests were performed at T-325 supersonic wind tunnel (available in the ITAM SB RAS) [25, 26]. Meanwhile, the permeable porous coating on the model surface cannot avoid natural roughness [27]. This roughness declines the positive effect from heavy gas injection (normally roughness destabilizes the boundary layer flow). Therefore, the further development of theoretical approach [20–24] in studying of possibility and feasibility in application of a sublimating coating (with low roughness) for control of flow stability and transition in the boundary layer looks logical and promising. This paper presents the first results of a theoretical study on stability of a supersonic flat-plate boundary layer in conditions of surface sublimation.

1. Boundary layer equations

Here we consider a model of a flat plate in a compressible gas (air) flow. It is assumed that the model surface is coated with a substance capable for sublimation at moderate temperatures (i.e., a solid-gas phase transition occurs skipping the melting stage). In this situation, the vapor of sublimation material with molecular mass m_2 (which is an admixture to the main gas with molecular mass m_1) travels from the model surface into the boundary layer of the main gas stream. We assume that the process of sublimation occurs rather slowly, hence the surface geometry remains unchanged while modeling. Under conditions, the boundary layer flow is not a single-component flow anymore: it becomes a binary mixture boundary layer flow. The time-dependent dynamics of that kind of binary mixture of viscous heat-conducting gases can be described by a set of partial differential equations (see paper [8]). The study [20] took these general equations in approximation of local self-similarity and derived a set of equations for a steady 2D supersonic boundary layer of a binary mixture flow (with zero chemical reactions) (see also [23]). Those equations take into account diffusion of sublimating material vapor across the boundary layer and take the following form:

$$\frac{d}{dy}\left(\mu\frac{dU}{dy}\right)+F\frac{dU}{dy}=0,\quad \frac{dq}{dy}=F\frac{dh}{dy}+(\gamma-1)\mathrm{M}_\mathrm{e}^2\mu\left(\frac{dU}{dy}\right)^2, \tag{1}$$

$$\frac{dj_1}{dy}=F\frac{dc_1}{dy},\quad q=-\lambda\frac{dT}{dy}+(h_1-h_2)j_1,\quad j_1=-\rho D_{12}\frac{dc_1}{dy},$$

where $y=y^*/\delta$ is a coordinate normal to the wall, $\delta=\sqrt{x\mu_\mathrm{e}/U_\mathrm{e}\rho_\mathrm{e}}$ is the Blasius length scale (it describes the boundary layer thickness over a flat plate), x is a streamwise coordinate (the coordinate origin is matched to the leading edge of the plate), $q(y)=\dfrac{\sqrt{x\mu_\mathrm{e}/U_\mathrm{e}\rho_\mathrm{e}}}{\mu_\mathrm{e}h_\mathrm{e}}q^*$ is the total heat flux across the boundary layer, c_1 is the foreign gas (vapor) mass concentration, $j=j^*\dfrac{\sqrt{x\mu_\mathrm{e}/U_\mathrm{e}\rho_\mathrm{e}}}{\mu_\mathrm{e}}$ is the diffusion-based mass flowrate of gas mixture across the layer, $U=\dfrac{2}{\rho}\cdot\dfrac{dF}{dy}$ is the streamwise velocity (in the freestream direction), F is the stream function, $h=h^*/\left(C_{p2}T_\mathrm{e}\right)$ is the enthalpy of binary mixture, $T=T^*/T_\mathrm{e}$ is the temperature, C_{p2}, C_{p1} are the specific heats of the primary gas (air) and the foreign vapor, correspondingly, $\mu=\mu^*/\mu_\mathrm{e}$ is the viscosity coefficient for the binary mixture, $\lambda=\lambda^*/\left(\mu_\mathrm{e}C_{p2}\right)$ is the thermal conductivity coefficient, $D_{12}=\rho_\mathrm{e}D^*_{12}/\mu_\mathrm{e}$ is the binary diffusion coefficient. Here the superscript asterisk stands for dimensional variables, while the symbols without asterisk are dimensionless variables. The subscript "e" describes the (dimensional) values taken at the boundary layer outer edge.

The boundary conditions for the sublimation surface are the following:

$$U(0)=0,\quad F(0)=-f_\mathrm{w},\quad f_\mathrm{w}=\frac{G_\mathrm{w}}{\rho_\mathrm{e}U_\mathrm{e}}\mathrm{Re}=\frac{\rho_\mathrm{w}V_\mathrm{w}}{\rho_\mathrm{e}U_\mathrm{e}}\mathrm{Re},$$

$$Q+G_\mathrm{w}(h-h_1)_\mathrm{w}+\left[-\lambda\left(\frac{dT}{dy}\right)+(h_1-h_2)j_1\right]_\mathrm{w}=0, \tag{2}$$

$$f_\mathrm{w}\left(1-c_{1,\mathrm{w}}\right)=-\rho_\mathrm{w}D_{12,\mathrm{w}}\left(\frac{\partial c}{\partial y}\right)_\mathrm{w},$$

where G_w is the mass flowrate for vapor from the sublimation surface, $Q = H_{sg} G_w$ is the energy consumed for coating evaporation, H_{sg} is the sublimation enthalpy (solid→gas), $\mathrm{Re} = \rho_e U_e \delta / \mu_e = \sqrt{\mathrm{Re}_1 x}$ is the Reynolds number calculated from the Blasius scale. The subscript "w" describes the parameters taken for the solid surface.

The boundary conditions at the boundary layer outer edge are the following:

$$(U, T) \to 1, \quad c_1 \to 0 \quad \text{at} \quad y \to \infty. \tag{3}$$

The mass flowrate of vapor from the surface can be calculated with the Knudsen-Langmuir equation [28]:

$$G_w = a_1 \frac{P_1^{sat} - P_1}{\sqrt{2\pi R T_w / m_1}}. \tag{4}$$

Obviously, the rate G_w depends on the difference between the saturation pressure for sublimant vapor P_1^{sat} at wall temperature T_w and partial pressure of substance vapor directly above the surface P_1 $(y \to +0)$. Here a_1 is an accommodation coefficient.

The saturated vapor pressure as a function of coating temperature can be found from the Clausius–Clapeyron equation [28]:

$$\ln\left(\frac{P_1^{sat}}{P_{TP,1}}\right) = \frac{H_{sg} m_1}{R}\left(\frac{1}{T_{TP,1}} - \frac{1}{T_w}\right), \tag{5}$$

where $P_{TP,1}$, and $T_{TP,1}$ are pressure and temperature for the triple point of the sublimating material. The partial pressure of vapor is calculated by formula $P_1 = \dfrac{c_1 m_2}{m_1 + (m_2 - m_1) c_1} P$.

It was shown in papers [21–24] that the key parameter affecting the properties of a binary gas boundary layer is the dimensionless injection coefficient f_w (2). To provide the self-similarity of the boundary-value problem (1)–(3), we have to satisfy the condition of a constant injection coefficient over the streamwise coordinate: $f_w = \mathrm{const}(x)$. In a case of a slow dependency $f_w = f_w(x)$, the concept of local self-similarity is applied to the system (1)–(3) for every step on the streamwise coordinate *x*. To provide a large value for the control coefficient f_w in formula (2), the temperature of the sublimating coating should be kept close to the triple point (see equations (4) and (5)). In the present study, this heating of surface is ensured by the increase of the flow stagnation temperature T_0.

The key coefficients (viscosity coefficient, thermal conductivity of components, diffusion coefficient for foreign vapor) were calculated using the model of Lennard–Jones in the framework of kinetic theory [29]:

$$\mu_i = 2.6693 \cdot 10^{-6} \frac{\sqrt{T m_i}}{d_i^2 \Omega^{(2,2)}}, \quad \lambda_i = 0.0833 \frac{\sqrt{T/m_i}}{d_i^2 \Omega^{(2,2)}},$$

$$D_{12} = 1.858 \cdot 10^{-7} \frac{\sqrt{T^3 \left(1/m_1 + 1/m_2\right)}}{P d_{12}^2 \Omega^{(1,1)}},$$

where d_i are the collision diameters for molecules, i = 1, 2; $\Omega^{(1,1)}$ and $\Omega^{(2,2)}$ are the collision integrals. The dimensions for the coefficients are as follows: μ_i [kg/(m·s)]; λ_i [W/(m·K)]; D_{12} [m^2/s]. Viscosity and heat conductivity for the binary mixture are calculated by formulas

from [30]. The Euken correction factor was considered in calculating the thermal conductivity of polyatomic gases.

In the present paper, the boundary-value problem for boundary layer equations for the case of a binary mixture flow (1)–(3) was numerically integrated using the Runge–Kutta method with the fourth order of accuracy. The shooting method and the nested Newtonian iterations were applied to satisfy the boundary conditions. All the boundary layer equations, boundary conditions, and numerical methods have been presented previously in paper [31].

2. Linear stability equations

The linear stability theory for the boundary layer of the binary gas mixture was developed and presented in [23]. After linearization of dimensionless equations of motion for a viscous heat-conducting binary gas mixture written for wave-like disturbances $\mathbf{q}(x,y,z,t) = \tilde{\mathbf{q}}(y)\exp\left(i(\alpha x+\beta z-\alpha Ct)\right)$ in the approximation of locally parallel base-flow, we derive the following set of ordinary differential equations:

$$i\alpha(U-C)\tilde{\rho}+\frac{d\rho}{dy}\tilde{v}+\rho\left(i(\alpha\tilde{u}+\beta\tilde{w})+\frac{d\tilde{v}}{dy}\right)=0,$$

$$\rho\left(i\alpha(U-C)\tilde{u}+\frac{dU}{dy}\tilde{v}\right)=-\frac{i\alpha\tilde{p}}{\gamma_{\mathrm{e}}\mathrm{M}_{\mathrm{e}}^2}+\frac{\mu}{\mathrm{Re}}\cdot\frac{d^2\tilde{u}}{dy^2},\quad \rho i\alpha\left(U-C\right)\tilde{v}=-\frac{1}{\gamma_{\mathrm{e}}\mathrm{M}_{\mathrm{e}}^2}\cdot\frac{d\tilde{p}}{dy},$$

$$\rho i\alpha(U-C)\tilde{w}=-\frac{i\beta\tilde{p}}{\gamma_{\mathrm{e}}\mathrm{M}_{\mathrm{e}}^2}+\frac{\mu}{\mathrm{Re}}\cdot\frac{d^2\tilde{w}}{dy^2},\quad i\alpha\left(U-C\right)\tilde{c}+\frac{dc}{dy}\tilde{v}=\frac{\mu}{\mathrm{Re}\,\mathrm{Sm}}\cdot\frac{d^2\tilde{c}}{dy^2},\tag{6}$$

$$\rho\left(i\alpha\left(U-C\right)\tilde{h}+\frac{dh}{dy}\tilde{v}\right)=\frac{\gamma_{\mathrm{e}}-1}{\gamma_{\mathrm{e}}}i\alpha\left(U-C\right)\tilde{p}+\frac{\mu}{\mathrm{Re}\,\mathrm{Pr}}\cdot\frac{d^2\tilde{h}}{dy^2}+\frac{\mu}{\mathrm{Re}}\left(h_1-h_2\right)\left(\frac{1}{\mathrm{Sm}}-\frac{1}{\mathrm{Pr}}\right)\frac{d^2\tilde{c}}{dy^2},$$

where (α,β) are the streamwise and spanwise wave numbers, $\omega=\alpha C=\omega^*\delta/U_{\mathrm{e}}=$ $=2\pi f\delta/U_{\mathrm{e}}$ is the dimensionless frequency of disturbance, f is the frequency (Hz), which is related to the reduced frequency Ω through the formula $\Omega=2\pi f\mu_{\mathrm{e}}/\rho_{\mathrm{e}}U_{\mathrm{e}}^2$, $\mathrm{Pr}=\mu C_p/\lambda$ is the Prandtl number, $\mathrm{Sm}=\mu/\rho D_{12}$ is the Schmidt number, $\tilde{\mathbf{q}}(y)=(\tilde{u},\tilde{v},\tilde{w},\tilde{p},\tilde{h},\tilde{c})^{\mathrm{T}}$ are the amplitudes of fluctuations for three velocity components, pressure, enthalpy, and foreign gas concentration, correspondently. For the analysis of the spatial stability problem, it is assumed that ω and β are real numbers, and $\alpha=\alpha_{\mathrm{r}}+i\alpha_{\mathrm{i}}$ is a complex number. The imaginary part of the streamwise wavenumber $\left(-\alpha_{\mathrm{i}}>0\right)$ is the spatial amplification rate of disturbances. Obviously, system (6) can be transformed to a set of ten ordinary differential equation of the first-order. This system can be solved under ten uniform boundary conditions:

$$\left(\tilde{u},\tilde{v},\tilde{w},\tilde{h},f_{\mathrm{w}}\tilde{c}+\rho_{\mathrm{w}}D_{12}\frac{d\tilde{c}}{dy}\right)=0\quad\text{at } y=0,\quad\left(\tilde{u},\tilde{v},\tilde{w},\tilde{h},\tilde{c}\right)\to 0\quad\text{at } y\to\infty.\tag{7}$$

The integration of the eigenvalue problem (6) and (7) was performed using the orthonormalization numerical method [4, 8]. Here the wavenumber $\alpha=\alpha_{\mathrm{r}}+\mathrm{i}\alpha_{\mathrm{i}}$ is an eigenvalue of the problem (6) and (7) with the maximum value of $-\alpha_{\mathrm{i}}$. More details on stability equations and numerical methods are available in [23].

3. Calculation results

Calculations for the boundary layer were performed for airflow past a flat plate at the Mach number M = 2. It was assumed that the model surface is coated with a substance suitable for pure sublimation at a moderate temperature (no other complex phenomena, e.g.,

Table

Variants of parameters for calculating the boundary layer profiles (see Fig. 1)

No	T_0, K	T_w, K	Re_1, 10^6/m
1	290	266	6.35
2	315	290	5.67
3	342	310	5.07
4	361	320	4.71
5	392	330	4.22
6	450	340	3.53
7	500	345	3.08
8	580	350	2.56

chemical reaction, dissociation, and ionization). This pattern is typical for substances like dry ice, camphor, iodine. In this paper, we consider a supersonic boundary layer above a naphthalene-coated ($C_{10}H_8$) plate. This chemical substance has the following set of thermophysical properties: $\frac{m_1}{m_2} = \frac{128.17}{28.96} \approx 4.4$, $C_{p1} = 165.7$ J/(mol·K), $H_{sg} = 72.6$ kJ/mol [32], $T_{TP,1} = 353.4$ K, $P_{TP,1} = 1060$ Pa [33]. Note that enthalpy for sublimation is a big value. By estimates based on those parameters, the solid-gas phase transition for one mole of naphthalene (sublimation at steady temperature) is equivalent to the energy required for heating of one mole $C_{10}H_8$ by temperature difference $\Delta T = H_{sg}/C_{p1} = 438$ degrees. The collision diameter of naphthalene molecules (needed for calculation of transport properties of binary gas mixture) is $\sigma_1 \approx 6.45$ Å [34]. The choice of naphthalene in this study (except its favorable thermophysical properties) is the fact that this hydrocarbon is cheap and available.

For all presented results, we take the stagnation pressure $P_0 = 0.5$ bar, which is routine for boundary layer transition experiments performed at T-325 supersonic wind tunnel (owned by ITAM Siberian Branch of Russian Academy of Sciences) [25, 26]. In this study, we performed calculations for a supersonic boundary layer above a flat plate and its linear stability while increasing the mass flowrate of naphthalene vapor G_w. The flowrate was increased due to growth of coating temperature T_w, which is achieved through the growth of flow stagnation temperature T_0. The variants were calculated with the adiabatic-wall boundary conditions (2) and condensed into the Table. The column titles are the following: number of variant (the same numbers are used for denoting the curves in Figs. 1, 3–5), flow stagnation temperature T_0, surface temperature T_w (temperature of adiabatic wall obtained after numerical integration of problem (1)–(3) at a given value of T_0), and unit Reynolds number Re_1.

The presentation for computation results begins with the properties of the base flow. Figure 1 presents the calculated profiles for a boundary layer: dimensionless streamwise velocity $U = U(y)$ (Fig. 1*a*), temperature $T = T(y)$ (Fig. 1*b*), density $\rho = \rho(y)$ (Fig. 1*c*), and concentration of vapor $C_{10}H_8$ $c_1 = c_1(y)$ (Fig. 1*d*) — for different values of stagnation temperature T_0. One can see that the growth of T_0 brings a slight decrease in the boundary layer thickness in the dimensionless format (Fig. 1*a*). We also note that the growth in T_0 leads to the growth of the viscosity of gas mixture and, hence, to a higher thickness δ. The temperature profile $T = T(y)$ (plotted in Fig. 1*b*) demonstrates a significant decrease in the dimensionless temperature near the wall $T(0)$ with a higher T_0, although the dimensional value of wall temperature increases (see Table). A moderate decline in the boundary layer thickness can be observed in the temperature profiles also. The density profiles (Fig. 1*c*) demonstrate a significant change: while the growth of temperature T_0 from 290 to 580 K the gas mixture density at

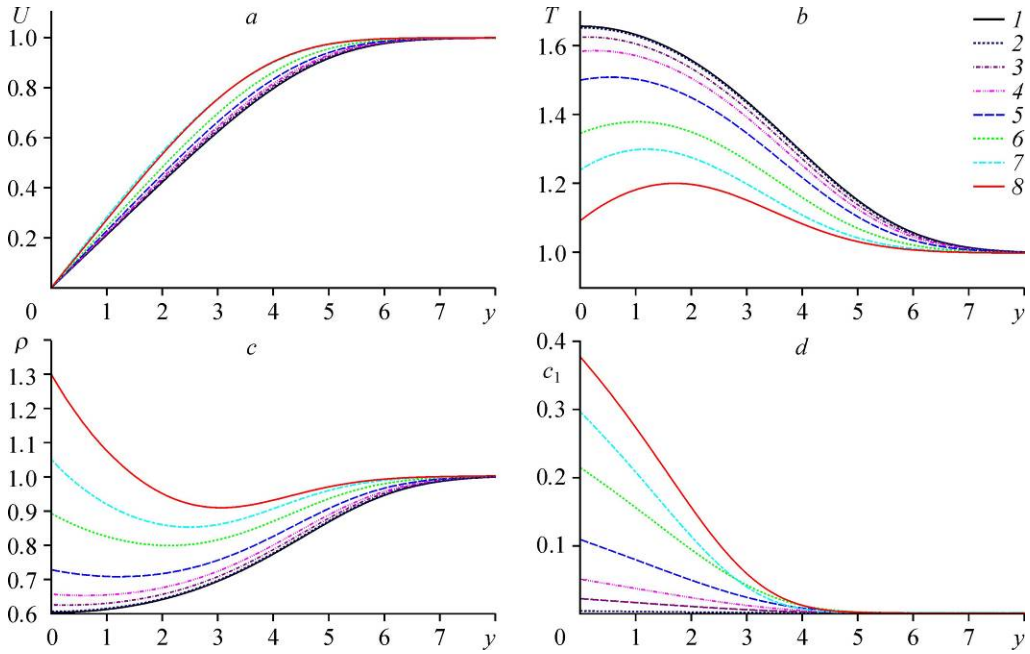

Fig. 1. Profiles for a boundary layer of a binary mixture flow (air + $C_{10}H_8$ vapor): dimensionless velocity $U = U(y)$ (*a*), temperature $T = T(y)$ (*b*), density $\rho = \rho(y)$ (*c*), admixture concentration $c_1 = c_1(y)$ (*d*) at different values of stagnation temperature T_0. See descriptions for cases *1*–*8* in the Table.

the wall $\rho_w = \rho(y = 0)$ increases more than twice. Figure 1*d* shows that the growth of mass flowrate from sublimation (induced by growth of T_0) increases the admixture concentration at the wall $c_{1,w} = c_1(0)$. However, concentration $c_1(y)$ decreases rapidly with distance from the surface. At the outer edge of the boundary layer (defined from the velocity profiles – see Fig. 1*a*), this concentration becomes negligibly low. Thus, the injection of vapor is low for the tested range of parameters – because the admixture (evaporated naphthalene) does not go beyond the boundary layer.

Figures 2*a* and 2*b* demonstrate the dimensional mass flowrate of the sublimation substance G_w and dimensionless injection coefficient f_w as a function of streamwise coordinate x at different values of the unit Reynolds number Re_1. The iterative solution of problem (1)–(3)

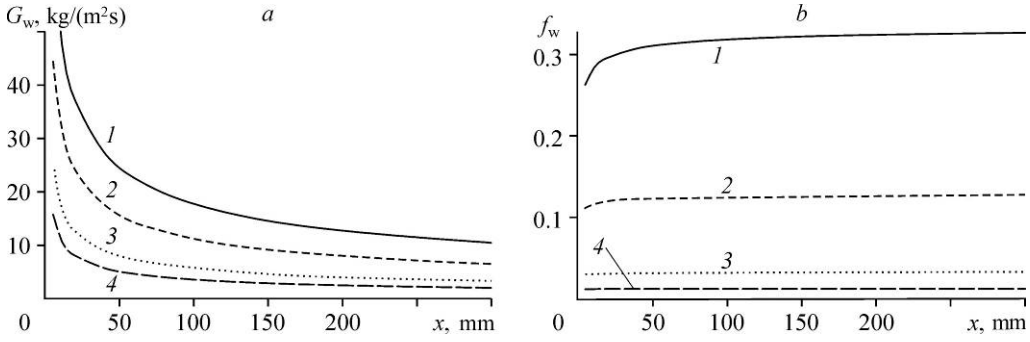

Fig. 2. Sublimation mass flow rate (dimensional) from the surface G_w (*a*) and dimensionless injection factor f_w (*b*) vs. streamwise coordinate x at different values of unit Reynolds number. $\mathrm{Re}_1 \cdot 10^{-6} = 2.5$ (*1*), 6.6 (*2*), 25.4 (*3*), 63.6 (*4*) m^{-1}.

for the base-flow demonstrates that G_w is not a constant, but it declines downstream (Fig. 2*a*). The sublimation mass flowrate decreases with a growth of the unit Reynolds number. On the contrary, the injection coefficient f_w depends on coordinate x only near the leading edge (Fig. 2*b*), but further downstream it approaches a steady level (independent of the streamwise coordinate for the tested range of parameters). That is the boundary layer in the downstream motion reconfigures rapidly and approaches a self-similarity mode. Thus, Fig. 2*b* illustrates the justification for using the local self-similarity approximation (1) that is used here for calculating a supersonic boundary layer above the surface with sublimation. Here we take a typical value of injection parameter (Fig. 2*b*) as $f_w \approx 0.2$. Then, using the definition for f_w from (2), we obtain that $\rho_w V_w << \rho_e U_e$, since for the region of linear instability we have Re > 500. Taking the ratio $\rho_w / \rho_e \approx 1$ (Fig. 1*c*), we have $V_w / U_e << 1$, and this is a justification for the parallel flow approximation used here for calculation of flow stability.

Figure 3 shows the results of calculation for linear stability. The plotting is a spatial amplification rate of two-dimensional (2D, $\beta = 0$) disturbances as a function of frequency for different values of flow stagnation temperature T_0 at x = 100 mm. The curves are labeled with numbers of simulation variants from the Table. Curve *1* corresponds to calculation of boundary layer stability for the case of the lowest stagnation temperature (influence of sublimation on stability is negligible). For this case, the unstable frequency range is $6 < f < 25$ kHz, while the maximal disturbance amplification rate $-\alpha_{i,max} \approx 4.6$ m^{-1} belongs to the disturbance with the frequency $f_{max} \approx 16.5$ kHz. At higher stagnation temperatures, we observe a steady decrease in the amplification rate for the entire frequency range and also a decrease in f_{max}. Already at the temperature T_w = 330 K (T_0 = 392 K, variant #5 from the Table), the boundary layer is completely stabilized. The disturbance growth rate becomes negative $(-\alpha_i < 0)$. This means that linear two-dimensional disturbances are stable and their amplitude decreases in downstream direction. The further growth in T_0 causes a monotonous decline in amplification rate for the entire frequency range (curves *6*–*8* in Fig. 3).

Figure 3 presents calculations for the disturbance growth rate only for 2D disturbances which are not the fast-growing disturbances for a boundary layer at Mach number M = 2. Now we address the characteristic of linear stability in a supersonic boundary layer for the case of 3D disturbances. Figures 4*a* and 4*b* present the diagrams of boundary layer stability as contour lines of spatial growth rates at the coordinate plane: angle of orientation of the wavevector $\chi = \arctan(\beta/\alpha_r)$ – dimensional frequency f [kHz]. Here we have presented the results in dimensional format foreseeing their use in experiments. The corresponding dimensionless values Ω and Re (see notes to formulas (2) and (6)) can easily be calculated from the Table data.

These computations were performed for the value of streamwise coordinate x = 100 mm and flow stagnation temperature T_0 = 392 K (variant #5 in the Table). The region at the plane (χ, f), which is restricted by curve $-\alpha_i = 0$, is the instability range ($-\alpha_i > 0$). Amplitude of disturbances with parameters from this area grows downstream. Figure 4*a* presents the stability diagram for a boundary layer on a flat plate for the case of zero sublimation. Figure 4*b* shows a similar plotting, but for a plate with naphthalene

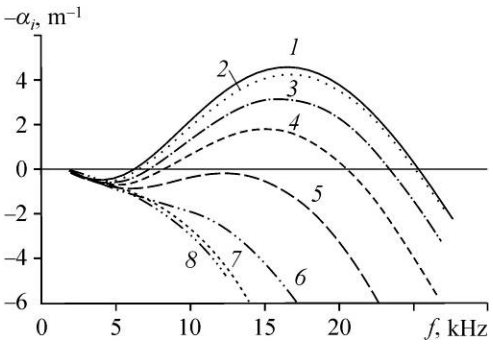

Fig. 3. Spatial amplification rates for 2D disturbances vs. frequency f at different stagnation temperatures T_0. See the legend for curves *1*–*8* in the Table.

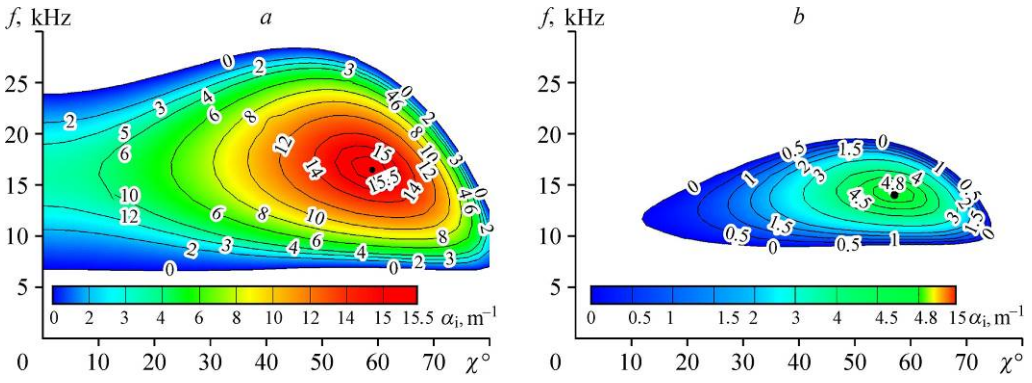

Fig. 4. Instability map for a supersonic boundary layer with induced 3D disturbances: spatial amplification rate contours $-\alpha_i = -\alpha_i(x, f)$ [m^{-1}] at the adiabatic surface at $T_0 = 392$ K, $x = 100$ mm without sublimation (*a*) and for sublimation of naphthalene coating at $T_w = 330$ K (variant #5 in the Table) (*b*).

coating. The color legends in the stability diagrams in Figs. 4*a* and 4*b* are identical to simplify the comparison of computational results. One can see that the instability range shrinks due to injection of heavy naphthalene vapor into the near-wall sublayer. With zero sublimation, the maximum amplification of disturbances ($-\alpha_{i,max} \approx 15.7$ m^{-1}) occurs at $f_{max} \approx 16$ kHz and $\chi_{max} \approx 59^\circ$ (Fig. 4*a*). For the case of naphthalene sublimation, this parameter is lower: $-\alpha_{i,max} \approx 4.9$ m^{-1} at $f_{max} \approx 14$ kHz and $\chi_{max} \approx 57^\circ$ (Fig. 4*b*). The 2D disturbances ($\chi = 0$), which are slightly unstable at zero injection, become completely stable under impact of naphthalene vapor injection into the boundary layer, as shown in Fig. 3. Here the original range of unstable frequencies $7 < f < 28$ (Fig. 4*a*) shrinks to the range $9 < f < 19$ (Fig. 4*b*) due to stabilization at higher frequencies. Thus, the maximum value of amplification rate $-\alpha_{i,max} \approx 15.7$ at the chosen coordinate x decreases by factor of 3.2 only due to sublimation of naphthalene coating. The depicted change in the boundary layer stability diagrams (transition Fig. 4*a* → Fig. 4*b*) due to surface sublimation at the adiabatic wall demonstrates benefits in stabilization of the boundary layer.

Figure 5 offers comparison of the rates of 3D disturbance growth at the chosen frequency $f = 15$ kHz (see Fig. 4) as a function of wavevector orientation χ (at different values of T_0). The rates of fluctuation growth at the sublimation surface are depicted by dashed curves, while the case of zero sublimation is depicted by solid curves. One can see that at the lowest value of stagnation temperature, the effect of sublimation is minimal (dashed and solid curves almost coincide). The disturbance with $\chi \approx 60^\circ$ has the highest growth rate $-\alpha_{i,max} \approx 21$ m^{-1}and this is typical of a supersonic boundary layer. One can see that the growth of stagnation temperature causes a steady decline in the growth increment for all parameters $0 \le \chi < 80^\circ$. Comparing the solid and dashed curves of

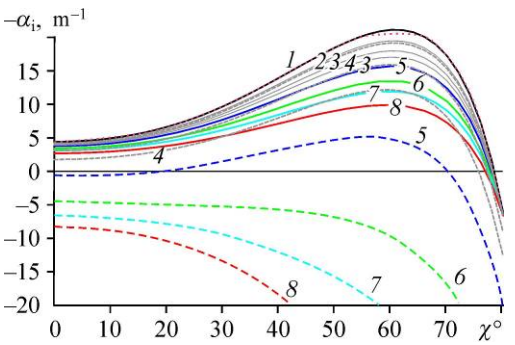

Fig. 5. Spatial amplification rate $-\alpha_i$ for the case of 3D disturbance as a function of angle χ at different values of T_0 (numbering according to Table) at $f = 15$ kHz and $x = 100$ mm. Dashed lines — for surface with sublimation, solid lines — no sublimation.

one color and with the same ordinal number from Fig. 5, we can judge about the influence of naphthalene coating sublimation on the growth rate of unstable disturbances. Here the growth in stagnation temperature from $T_0 = 290$ K to $T_0 = 580$ K at the absence of sublimation (solid curves *1*–*8*) reduces the maximum amplification rate down to $-\alpha_{i,max} \approx 10$ m^{-1}, i.e., almost twice. Meanwhile, the boundary layer over a sublimating coating is stable completely $\left(-\alpha_{i,max} < 0\right)$ at the stagnation temperature about $T_0 \approx 420$ K (in between the curves *5* and *6* in Fig. 5).

Figures 6*a* and 6*b* present the following stability maps: spatial amplification rate contours for most unstable 3D disturbances ($\chi = 60°$). These contours are plotted in coordinates: streamwise coordinate x and the dimensional frequency f [kHz]. As previously, calculations were performed for temperature $T_0 = 392$ K (variant #5 from the Table). Similar to the data presented in Figs. 4*a* and 4*b*, the plotting in Fig. 6*a* demonstrates a map with zero sublimation, while Fig. 6*b* shows a similar case for a plate with naphthalene coating. Comparison between Figs. 6*a* and 6*b* reveals that evaporation of naphthalene (and heavy vapor injection into the boundary layer) reduces the sizes of instability zone. The frequency range for instability is reduced almost twice due to suppression of high frequency disturbances. For the case of zero sublimation, the maximal growth rate $-\alpha_{i,max} \approx 18$ m^{-1} corresponds to the disturbance with frequency $f_{max} \approx 30$ kHz at $x \approx 40$ mm (Re ≈ 430) (Fig. 6*a*). Meanwhile, the plate with naphthalene coating has the maximum increment $-\alpha_{i,max} \approx 5$ m^{-1} for the disturbance with frequency $f_{max} \approx 10$ kHz at $x \approx 150$ mm $\left(\mathrm{Re} \approx 800\right)$ (Fig. 6*b*). The critical Reynolds number that corresponds to loss of stability (calculated from the Blasius length scale) increases from $\mathrm{Re}_c \approx 250$ to $\mathrm{Re}_c \approx 410$ ($T_w = 330$ K, variant # 5 in the Table). The flow stabilization is obvious: the dimensional maximum amplification rate $-\alpha_{i,max}$ drops almost triple for the case of a surface with sublimation. This is not the utmost limit: for a flow with a higher stagnation temperature, this gain in stabilization can be stronger. Thus, the stability maps calculated from the linear stability theory (Fig. 6*a*, 6*b*) demonstrate the cumulative stabilizing influence of sublimating naphthalene ($C_{10}H_8$) coating on the stability of a supersonic boundary layer. Now we can illustrate this conclusion through calculation of the disturbance amplification curves.

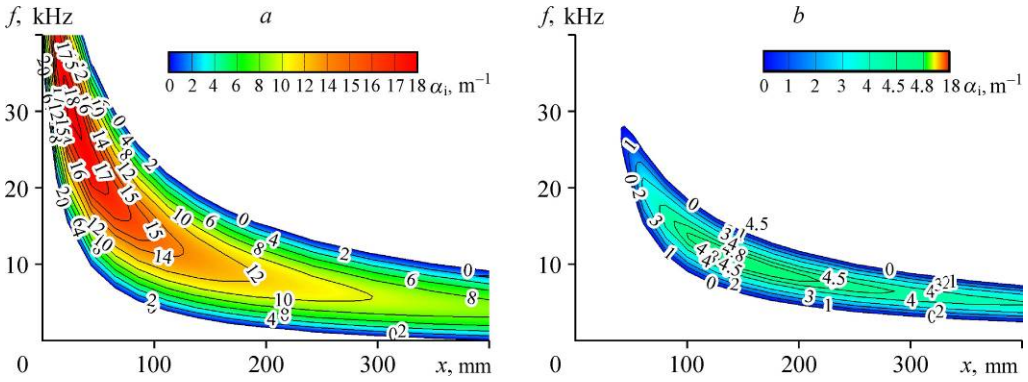

Fig. 6. Instability map of a supersonic boundary layer for situations of highly unstable 3D disturbances with $\chi = 60°$: isolines for spatial growth rate $-\alpha_i = -\alpha_i(x, f)$ [m^{-1}] at the adiabatic surface at temperature $T_0 = 392$ K without sublimation (*a*) and for sublimating naphthalene coating at $T_w = 330$ K (variant # 5 in the Table) (*b*).

The linear stability theory offers an opportunity of estimating the position of laminar-turbulent transition using a well-known method e^N [35]. According to this method, a position of laminar-turbulent transition is defined by controlling the disturbance amplification coefficient when it reaches a threshold value e^N, where the *N*-factor calculated as the integral of local disturbance growth rate for chosen frequencies: $N_{\mathrm{t}} = -\int_{\mathrm{Re}_0}^{\mathrm{Re}_{\mathrm{t}}} 2\,\mathrm{Im}(\alpha)\, d\,\mathrm{Re}$. Initially, this method was developed for 2D boundary layers of incompressible fluid. After comparing the *N*-factors calculated by the linear stability theory and experimental data for actual transition it was found that this transition occurs at $N_{\mathrm{t}} \approx 10$. The benefit of using the e^N method for theoretical estimation of transition position consists precisely in the assumption that $N_{\mathrm{t}} = \mathrm{const}$. Numerous subsequent endeavor of using this method for boundary layer under different conditions demonstrated that at low levels of external disturbances, this method works for estimations and prognosis of this kind of transition.. However, the specific value of *N*-factor in various situations (for different types of instability) was different: $7 < N_{\mathrm{t}} < 11$. In addition it was found that for super- and hypersonic boundary layers, this *N*-factor depends on the free-flow disturbance level in the test-section of a supersonic wind tunnel. For example, N_{t} decreases from 8.1 to 2.6 while the level of external disturbances increases from 0.1 % to 1 % [36]. Here we present calculations by e^N method for illustrating the idea of stabilizing action of a sublimation coating for control of position of a laminar-turbulent transition without assigning a certain value for N_{t}, (which depends on noise level in a specific experimental facility).

Figures 7*a* and 7*b* present the calculations with the e^N method: we plotted the amplification curves for most fast-growing 3D disturbances ($\chi \approx 60^\circ$) with different frequencies as a function of Reynolds number. Calculations are presented for a plate without sublimation (Fig. 7*a*) and for a plate with naphthalene coating ($T_{\mathrm{w}} = 330$ K, see variant #5 in the Table) (Fig. 7*b*). These amplification curves were calculated for two frequency ranges: $30 \ge f \ge 2$ kHz (Fig. 7*a*) and $10 \ge f \ge 0.25$ kHz (Fig. 7*b*). Obviously, the *N*-factor, which actually is an envelope for those curves, increases monotonously in the downstream direction. Comparison of data in Fig. 7*a* and 7*b* demonstrates that the *N*-factor on the sublimating coating takes the same level as for the case without sublimation at the Reynolds numbers higher by the factor of 2.5. For example, $N_{\mathrm{t}} = 10$ is reached at $\mathrm{Re} \approx 4800$ for a flow without sublimation (Fig. 7*a*) and at $\mathrm{Re} \approx 12000$ for a flow over the naphthalene coating (Fig. 7*b*). Note also a growing frequency range shift to the lower values on the sublimation coating.

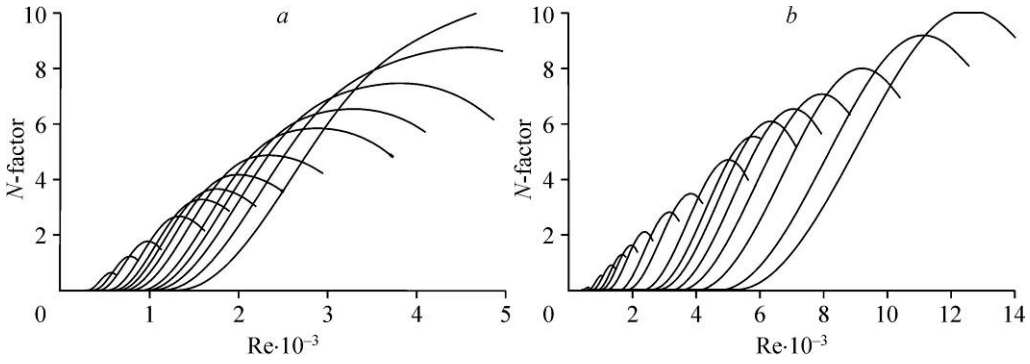

Fig. 7. Disturbance amplification curves calculated by e^N method for adiabatic surface at $T_0 = 392$ K without sublimation (*a*) and on naphthalene coating at $T_{\mathrm{w}} = 330$ K (variant #5 in the Table) (*b*).

Finally, it is worth to note that the visualization of a boundary layer above the naphthalene coating can be accomplished at the molar fraction of $C_{10}H_8$ about $1\cdot10^{-4}$ [19]. However our study has shown that a noticeable effect of sublimation on the boundary layer stability (under the described above conditions) can be obtained when the mass concentration of foreign vapors near the wall is by three orders of magnitude higher: $c_{l,w} > 20\,\%$ (see Fig. 4*b* and curves *5*–*8* in Figs. 1*d*, 3, 5). This paper also shows that this is quite realizable at rather high (although moderate) values of wall temperature T_w.

Conclusions

Base-flow and linear stability computations were performed for the boundary layer at Mach number 2 for the flat-plate with naphthalene ($C_{10}H_8$) coating. It was demonstrated that heavy vapors injection into a near-wall sublayer of the boundary layer (due to evaporation of coating material) increases the density of the binary-mixture boundary layer (air + naphthalene) near the sublimating surface. Calculation of linear stability for this modified flow has demonstrated the opportunity of reducing the local growth rates of linear wavy disturbances. This happens when the temperature of the surface increases up to the triple point temperature of $C_{10}H_8$. The calculations of the disturbance amplification curves (carried out in accordance with the e^N method based on the linear stability theory) have demonstrated the opportunity of significant stabilization for the boundary layer through initiating of sublimation. In particular, the Reynolds number for laminar-turbulent transition estimated by the e^N method becomes more than twice higher on the sublimation naphthalene coating in the flow with stagnation temperature of 392 K. This means a significant stabilization of a boundary layer and more than four-fold extension of the laminar flow span in a supersonic boundary layer over the naphthalene coating.

References

1. **G.A. Tirskii,** Hypersonic Aerodynamics and Heat Transfer of Reentry Modules and Planetary Probes, FIZMATLIT, Moscow, 2011.
2. **C.C. Lin,** The Theory of Hydrodynamic Stability, Cambridge University Press, 1955.
3. **L.M. Mack,** Boundary layer stability theory, Report 900-277 Rev. A., Pasadena, 1969.
4. **S.A. Gaponov and A.A. Maslov,** Development of Disturbances in Compressible Flow, Nauka, Novosibirsk, 1980.
5. **V.N. Zhigulev and A.M. Tumin,** Turbulence Onset. Dynamic Theory of Instability Excitation and Development in a Boundary Layer, Nauka, Novosibirsk, 1987.
6. **G.V. Petrov,** Boundary layer stability of a gas with chemical reactions on a catalytic surface, Combustion, Explosion and Shock Waves, 1974, Vol. 10, No. 6, P. 719–721.
7. **G.V. Petrov,** Stability of boundary layer of catalytically recombining gas volume, J. Appl. Mech. Tech. Phys., 1978, Vol. 19, No. 1, P. 32–35.
8. **S.A. Gaponov and G.V. Petrov,** Stability of the Boundary Layer with Nonequilibrium Gas Dissociation, Nauka, Novosibirsk, 2013.
9. **M.R. Malik and E.C. Anderson,** Real gas effects on hypersonic boundary-layer stability, Phys. Fluids A, 1991, No. 3, P. 803–821.
10. **G.K. Stuckert,** Linear stability of hypersonic, chemically reacting viscous flows, PhD thesis. Arizona State University, 1991.
11. **G.K. Stuckert and H.L. Reed,** Linear disturbances in hypersonic, chemically reacting shock layers, AIAA J. 1994, Vol. 32, P. 1384–1394.
12. **C.L.H. Chang, H. Vinh, and M.R. Malik,** Hypersonic boundary-layer stability with chemical reactions, AIAA Paper, 1997, No. 1997–2012.
13. **M.L. Hudson, N. Chokani, and G.V. Candler,** Linear disturbances in hypersonic, chemically reacting shock layers, AIAA J, 1997, Vol. 35, P. 958–964.
14. **H.B. Johnson, T.G. Seipp, and G. Candler,** Numerical study of hypersonic reacting boundary layer transition on cones, Phys. Fluids, 1998, Vol. 10, P. 2676–2685.
15. **C. Mortensen and X. Zhong,** Simulation of second-mode instability in a real-gas hypersonic flow with graphite ablation, AIAA J., 2014, Vol. 52, No. 8, P.1 632–1652.
16. **C. Mortensen and X. Zhong,** Real gas and surface-ablation effects on hypersonic boundary-layer instability over a blunt cone, AIAA J., 2016, Vol. 52, No. 3, P. 976–994.

17. **A.F. Charwat,** Exploratory studies on the sublimation of slender camphor and naphthalene models in a supersonic wind-tunnel, Memorandum RM-5506-ARPA. 1968.
18. **R.H. Radeztsky, M.S., Reiberta, and W.S. Saric**, Effect of isolated micron-sized roughness on transition in swept-wing flows, AIAA J., 1999, Vol. 37, No. 11, P. 1370–1377.
19. **C.S. Combs, N.T. Clemens, P.M. Danehy, and S.M. Murman,** Heat-shield ablation visualized using naphthalene planar laser-induced fluorescence, J. Spacecraft Rockets, 2017, Vol. 54, No. 2, P. 476–494.
20. **S.A. Gaponov and B.V. Smorodsky,** Laminar supersonic boundary layer of binary gas mixture, Vestnik Novosibirsk State University, 2016, Vol. 11, No. 1, P. 5–15.
21. **S.A. Gaponov and B.V. Smorodsky,** On stability of the supersonic boundary layer with a foreign gas injection, in: 18th Intern. Conf. on the Methods of Aerophysical Research, ICMAR-2016, Russia, Perm, 27 Jun.-3 Jul., 2016: AIP Conference Proceedings. 2016. Vol. 1770, S. l. P. 030047-1–030047-9.
22. **S.A. Gaponov and B.V. Smorodsky,** Supersonic boundary layer of binary mixture and its stability, Int. J. Mechanics, 2016, Vol. 10, P. 312–319.
23. **S.A. Gaponov and B.V. Smorodsky,** Control of supersonic boundary layer and its stability by means of foreign gas injection through the porous wall, Int. J. Theoret. Appl. Mech., 2016, Vol. 1, P. 97–103.
24. **S.A. Gaponov and B.V. Smorodsky,** Supersonic boundary layer under foreign gas injection and its stability, in: Proc. XXV Conf. on High-Energy Processes in Condensed Matter (HEPCM-2017): Dedicated to the 60th anniversary of the Khristianovich Institute of Theoretical and Applied Mechanics SB RAS, Russia, Novosibirsk, 5–9 Jun., 2017: AIP Conference Proceedings. S. l.: AIP Publishing: 1893. 2017. No. 1. P. 030087-1–030087-10.
25. **V.I. Lysenko, B.V. Smorodsky, Y.G. Ermolaev, S.A. Gaponov, N.N. Zoubkov, and A.D. Kosinov,** Experimental investigation of influence of heavy gas injection into supersonic boundary layer on laminar-turbulent transition, in: Proc. XXV Conference on High-Energy Processes in Condensed Matter (HEPCM-2017): Dedicated to the 60th anniversary of the Khristianovich Institute of Theoretical and Applied Mechanics SB RAS, Russia, Novosibirsk, 5–9 Jun., 2017: AIP Conference Proceedings. S. l.: AIP Publishing: 1893. 2017, P. 030077-1–030077-10.
26. **V.I. Lysenko, B.V. Smorodsky, Y.G. Ermolaev, and A.D. Kosinov,** Stability of supersonic boundary layer under the influence of heavy gas injection: experimental study, Thermophysics and Aeromechanics, 2018, Vol. 25, No. 2, P. 183–190.
27. **V.I. Lysenko, S.A. Gaponov, B.V. Smorodsky, Y.G. Ermolaev, A.D. Kosinov, and N.V. Semionov,** Combined influence of coating permeability and roughness on supersonic boundary layer stability and transition, J. Fluid Mech., 2016, Vol. 798, P. 751–773.
28. **Y.V. Polezhaev and F.B. Yurevich,** Thermal Protection, Energia, Moscow, 1976.
29. **J.O. Hirschfelder, C.F. Curtiss, R.B. Bird, and M.G. Mayer.** Molecular Theory of Gases and Liquids, Wiley, 1964.
30. **W.H. Dorrance,** Viscous hypersonic flow, McGraw-Hill, 1962.
31. **S.A. Gaponov and B.V. Smorodsky,** Influence of heavy gas blowing into the wall layer of supersonic boundary layer and its transition, Siberian J. Phys., 2019, Vol. 14, No. 1, P. 25–39.
32. **J.A. Dean,** Lange's Handbook of Chemistry, McGraw-Hill, N.Y., 1999.
33. **W.M. Haynes, D.R., Lide, and T.J. Bruno,** CRC Handbook of Chemistry and Physics. CRC Press. 2017.
34. **F. Li, J. Lee, and E.R. Bernstein,** Spectroscopy of naphthalene in simple molecular liquids, J. Phys. Chem., 1983, Vol. 87, No. 7, P. 1175–1180.
35. **J.L. Van Ingen,** A suggested semiempirical method for the calculation of the boundary layer transition region, VTH-74, Delft University of Technology, 1956.
36. **M.R. Malik,** Prediction and control of transition in supersonic and hypersonic boundary layers, AIAA J., 1989, Vol. 27, No. 11, P. 1487–1493.